Research Article | Vol. 28, No. 9 / 27 April 2020 / Optics Express 13516
Optics EXPRESS

Mo/Si multilayers sputtered onto inclined substrates: experiments and simulations

SHIZHUANG SUN,[1,2] BO YU,[1,3] TAO GUO,[1] SHUN YAO,[1] YU LIU,[1] WENYUAN DENG,[1] CHUN LI,[1] AND CHUNSHUI JIN[1,4]

[1]State Key Laboratory of Applied Optics, Changchun Institute of Optics, Fine Mechanics and Physics, Chinese Academy of Sciences, Changchun 130033, China
[2]University of Chinese Academy of Sciences, Beijing 100049, China
[3]yubodisan@126.com
[4]jincs@sklao.ac.cn

Abstract: We performed experiments involving the fabrication of Mo/Si multilayer coatings and established a model of the deposition process. The surface and interface roughness, surface power spectral density, layer structures, and coating reflectivity were characterized for different substrate inclination angles. The surface and interface roughness increase and the coating reflectivity decreases with an increase in the substrate inclination angle, especially for large angles (50–70°). The model was applied to explain this phenomenon, and a proposal to reduce the interfacial roughness caused by substrate inclination angles is presented.

1. Introduction

With the increase in the demand for high-speed computation at low power consumption rates, extreme ultraviolet lithography (EUVL) is seeing significant development. The process for depositing the Mo/Si multilayer coating on the EUV collector mirror is a critical step that has a determining effect on the output power, imaging quality, and working life of EUVL systems. Therefore, the optimization of the process for depositing the Mo/Si multilayer coating on the collector mirror should lead to further improvements in the performance of EUVL [1–6].

Theoretically, the EUV reflectance of Mo/Si multilayer coatings on collector mirror can be around 75% [2], but in practice the reflectance is lower than 69% and the reflectivity at the edge with large substrate inclination angle (about 50°) is reduced by about 2% compared to the reflectivity near the center [7–9]. The decrease of reflectivity at the edge is mainly caused by the increase of interfacial roughness of Mo/Si multilayer deposited at larger substrate inclination angle, as mentioned by Broadway et al. [10]. Therefore, the effects of the substrate inclination angle on the coating structure and its roughness should be elucidated if one wishes to improve the reflection efficiency of the coating.

Torrea et al. [11] performed magnetron sputtering experiments to study the deposition process of sputtering Ta atoms on inclined Si(100) substrates as well as the microstructures of the thus-deposited films; the maximum substrate inclination angle studied was 70°. Moreover, they established a 3D model to simulate the structures of the films grown for different substrate inclination angles. Trost et al. [7] studied the variations in the scattering characteristics of Mo/Si multilayer coatings formed on Si substrates with different inclination angles; in this case, the maximum substrate inclination angle investigated was 30°.

Voronov et al. [12] used ion-beam sputtering method to fabricated Mo/Si multilayers with different substrate inclination angles from 0° to 65° and present a continuum model for the growth of the nano-ripples, which is very useful for understanding the evolution of Mo/Si multilayer structures deposited at different inclination angles. In their experiment, the residual divergence of the deposition angles on the substrate was very small (7°) and there was no need to consider the distribution of incident angles. However, in our case Mo/Si multilayers are deposited on EUV

#390216 https://doi.org/10.1364/OE.390216
Journal © 2020 Received 11 Feb 2020; revised 20 Mar 2020; accepted 24 Mar 2020; published 20 Apr 2020

Optics EXPRESS

collector mirror by large-size planar magnetron sputtering source with angular and sputtering yield distribution of sputtered atoms [5,13,14], and it is necessary to consider the complicated wide distribution of incident angles and its influence on the growth of the multilayers.

Neither of these previous studies directly clarified the reasons for the decreased reflectivity of the coating at the edge of the collector mirror. Hence, in this work, we fabricated Mo/Si multilayer coatings by the magnetron sputtering method on Si substrates with inclination angles of 0, 20, 30, 40, 50, 60, and 70°. Atomic force microscopy (AFM) and transmission electron microscopy (TEM) were used to measure the surface roughness and image the cross-sectional structures, respectively, of the multilayer coatings. Further, the reflectivity of the multilayer coatings for wavelengths of 12–16 nm was measured using an extreme ultraviolet spectrometer.

The structure of Mo/Si multilayer coatings can be optimized by improving the coating process based on the results of previous experimental studies [1–8]. However, this is time consuming, requires extensive practical experience, and would lead to material wastage. These problems can be overcome by utilizing a simulation model. The kinetics Monte Carlo (KMC) method and the molecular dynamics (MD) method have been employed previously to simulate coating deposition processes [15]. Yang et al. [16] used the KMC method to simulate the growth of a Nickel thin film while Schneider et al. [17] applied the MD method to simulate the effects of the energy of the incident atoms on the deposition process with the aim of improving the coating density. In this study, we combined these two methods to develop a model that can be used to simulate the deposition of Mo and Si atoms on Si substrates.

The proposed model was used to simulate the structure of Mo/Si multilayer coatings and study the variations in the coating structure and surface roughness with changes in the inclination angle of the substrate. The process conditions, including the temperature and pressure of the deposition environment, deposition rate, and voltages applied to the Mo and Si targets as well as the substrate inclination angle were kept the same as those during the experiments. It was found that the changes in the surface power spectral density (PSD) and surface roughness with the substrate inclination angle as simulated using the model were similar to those observed experimentally, thus confirming the suitability of the model.

2. Modeling of deposition

Magnetron sputtering is a popular coating deposition method. In this section, we present a model for the magnetron sputtering deposition of Mo/Si multilayer coatings based on the physical processes involved: 1) the distribution of the incident sputtered particles and 2) their deposition on the substrate.

2.1. Distribution of incident sputtered particles

In order to determine the distribution of the sputtered particles incident on the substrate, we need to model the following three processes: a) magnetron discharging, b) plasma–target interaction, and c) transport of particles in processing gas.

2.1.1. Magnetron discharging

An Ar plasma is generally used to bombard the Mo/Si targets and generate the sputtered Mo/Si particles during the deposition process. Under the effect of magnetic and electric fields, the Ar plasma is made to move away from its initial direction and bombard the Mo and Si targets at high speed. The sputtering yield distribution of the Ar plasma as it comes in contact with the Mo/Si targets was calculated based on the shape of the target grove [18,19] in our model.

2.1.2. Plasma–target interaction

When the Ar plasma bombards the Mo and Si targets at a certain angle and energy, Mo and Si atoms get sputtered from the respective targets. This process is considered a plasma–target

Optics EXPRESS

interaction. The software programs SRIM [20] and TRIM [21,22] applying the binary collision method were used to model this process, in order to determine the angle and energy distributions of the sputtered Mo/Si atoms and the reflected Ar atoms [23]. The voltages applied to the Mo and Si targets were 350 and 600 V, respectively.

2.1.3. Transport of particles in processing gas

The software SIMTRA [23] was used to model the movement of the sputtered particles in processing gas in order to determine the incident angles and energy distributions of the sputtered Mo and Si atoms and the reflected Ar atoms as they arrived at the substrate.

The spatial positions of the Mo and Si targets and the inclined substrate during the simulations are shown in Fig. 1 which were similar to those used during the experiments. The distance between each target and the substrate is 12 cm, and the diameter of each target is 10 cm. The environment temperature and pressure were kept at 300 K and $6e^{-2}$ Pa, respectively. The voltages applied to the Mo and Si targets were 350 and 600 V, respectively. The working gas is Ar plasma.

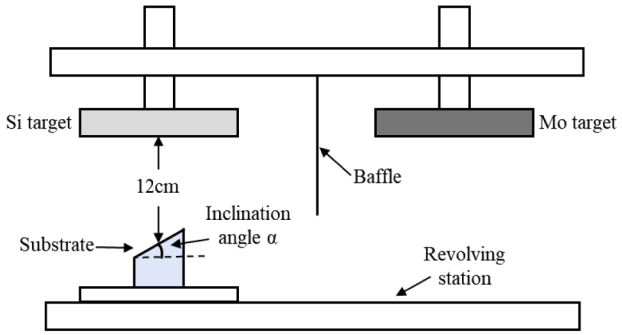

Fig. 1. Spatial positions of Mo and Si targets and inclined substrate.

Figures 2 and 3 show the incident angles and energy distributions of the Mo and Ar (Mo target) and Si and Ar (Si target) atoms arriving at the substrate, respectively. The substrate inclination angles were 0, 20, 40, 50, 60, and 70°.

It can be observed that the peak of the incident angle distribution moves to the left with the increase in the substrate inclination angle while the incident energy distribution remains almost unchanged; this is true for all three types of atoms (Mo, Si, and Ar). In addition, the peak of the incident energy distribution of the Ar atoms is higher than that of the Si atoms, indicating that the reflected Ar atoms also participate in the deposition process. The presence of these high-energy Ar atoms is one of the primary reasons to smooth the surface roughness of the coatings, as is explained next.

The incident angle and energy distributions of the atoms were taken as the initial conditions for the proposed deposition model.

2.2. Deposition of sputtered particles on substrate

The deposition of sputtered particles on substrate was simulated based on MD method and KMC method. The MD method was applied to investigate on the physical process of the high-energy sputtered atoms colliding with the substrate, similar to Yang's [24] study on the deposition of Ni/Cu multilayers and Luo's [25] work on the inclined deposition of Si thin films. Further, the KMC method was utilized to study the thermal diffusion process of atoms deposited on the substrate based on ADEPT and 2D KMC model [16, 26].

Optics EXPRESS

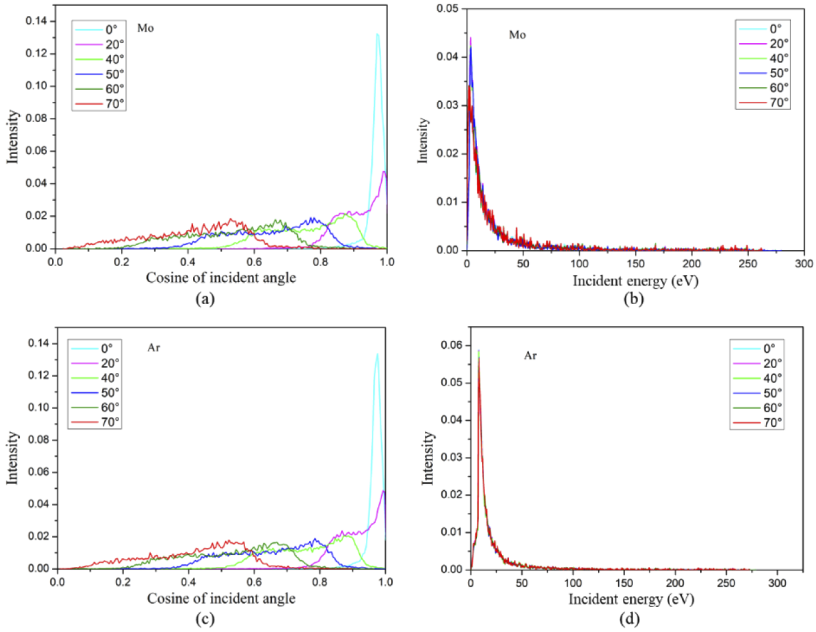

Fig. 2. Incident angles and energy distributions of Mo and Ar atoms (Mo target).

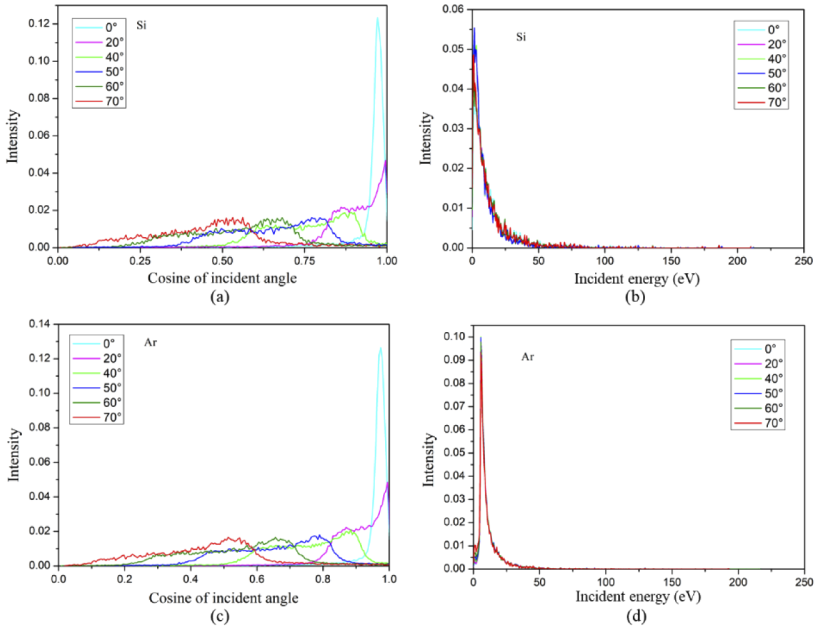

Fig. 3. Incident angles and energy distributions of Si and Ar atoms (Si target).

2.2.1. High-energy physical deposition

As the incident sputtered particles have a certain kinetic energy, they collide with the substrate and undergo reflection [27], resputtering [27], biased diffusion [28], and kinetic energy assisted diffusion [29–31] (shown in Fig. 4), determining the motion trajectory of the atoms and affecting

Optics EXPRESS

the deposited coating structure on the substrate. LAMMPS software containing MD method was practical used in our model to explore the four high-energy physical deposition processes.

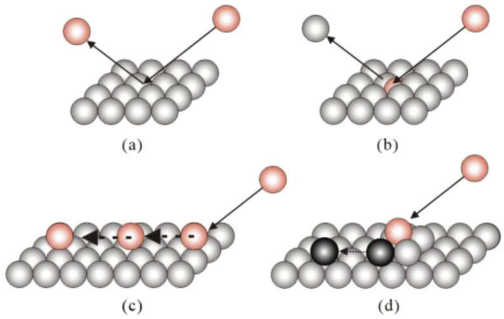

Fig. 4. High-energy physical deposition processes: (a) reflection, (b) resputtering, (c) biased diffusion, (d) and kinetic energy assisted diffusion

Four types of collision are considered in order to approximate the real multilayers deposition processes: 1) the collision of Mo atoms on a Mo substrate (Mo-on-Mo); 2) the collision of Mo atoms on a Si substrate (Mo-on-Si); 3) the collision of Si atoms on a Mo substrate (Si-on-Mo), and 4) the collision of Si atoms on a Si substrate (Si-on-Si). The four high-energy physical deposition processes all happen for these four types of collision. However, Since the sputtered Ar atoms are gaseous at working temperature, it is difficult for Ar to form thin films. Thus, we assumed that only kinetic energy assisted diffusion process happens when Ar atoms colliding with the substrate.

The reflection and resputtering probability, and biased diffusion distance in terms of incident angle and energy can be calculated for the four types of collisions by the MD method (the case of Mo-on-Mo is shown in Fig. 5). In addition, the angle and energy distribution of the reflection and resputtering atoms can be obtained as well [27, 28]. Therefore, the location of the sputtering atoms deposited on the substrate can be determined; afterwards, KMC method is used to account for the low-energy thermal diffusion processes discussed in the following.

2.2.2. Thermal diffusion

After the high-energy physical deposition processes, the atoms stop moving since their kinetic energy is consumed. However, the atoms would not remain at the same location; instead, they would jump stochastically to another position. This stochastic jumping is called thermal diffusion, which is one of the key factors affecting the film structure.

To calculate the thermal diffusion trajectory, it is necessary to compute the barrier energy for particle skipping. The potentials induced by the relative locations of the atoms during thermal diffusion can be computed using the modified embedded atom model (MEAM) method [32–34]. The nudged elastic band (NEB) method can then be employed to compute the barrier energy [2,35,36] based on the potentials. As per the principle of the NEB method, particle skipping occurs along the path with the lowest barrier energy and not along the shortest path. LAMMPS software applying MEAM and NEB method was used to calculate the barrier energy in our model.

If the thermal diffusion is assumed to conform to Boltzmann statistics, the jump probability for the atoms to the nearest neighbor empty site can be expressed as: $p_i = v_0 exp(-E_i/KT)$. Where, v_0 is the effective vibrational frequency, K is Boltzmann's constant, and T is the absolute temperature of the environment. E_i is the activation energy for jump i, which is the barrier energy acquired by the above mentioned MEAM and NEB methods.

Optics EXPRESS

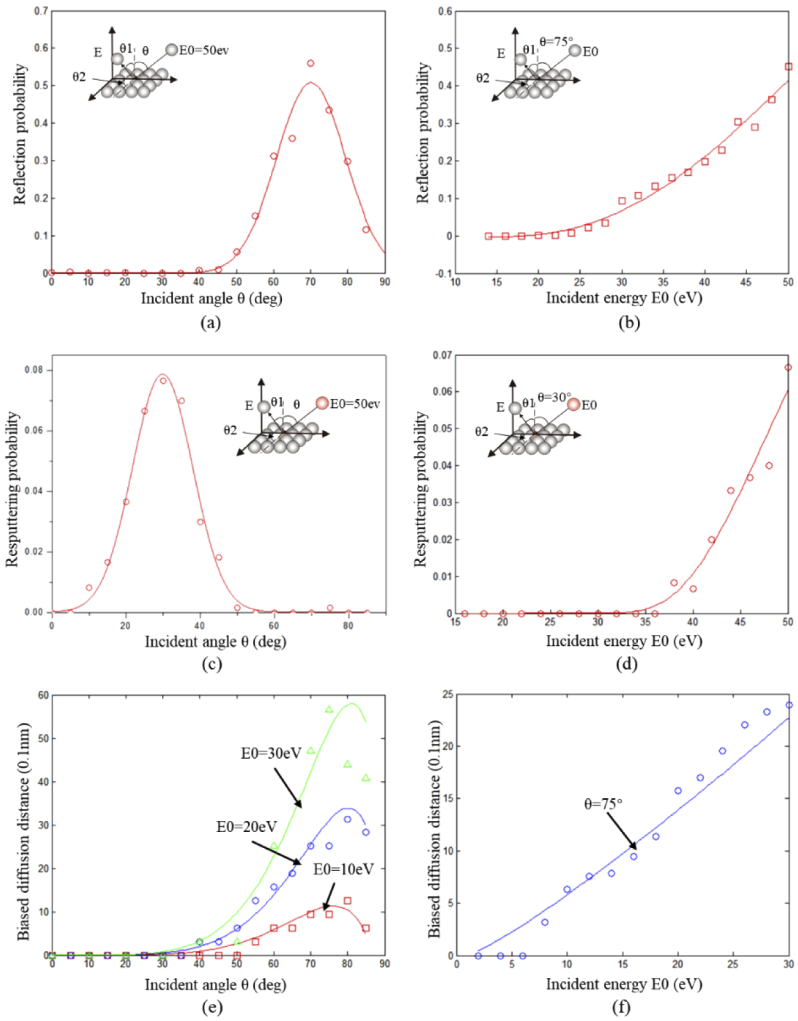

Fig. 5. Mo-on-Mo.(a) Reflection probability vs. incident angle, incident energy fixed at 50 eV. (b) Reflection probability vs. incident energy, incident angle fixed at 75°. (c) Resputtering probability vs. incidence angle, incident energy fixed at 50 eV. (d) Resputtering probability vs. incident energy, incident angle fixed at 30°. (e) Biased diffusion distance vs. incident angle, incident energies are 10, 20, and 30 eV. (f) Biased diffusion distance vs. incident energy, incident angle fixed at 75°.

KMC method is implemented to simulate the location changes of atoms under the thermal effect based on the jumpy probability p_i, and final film structure is thereby determined [16].

The incident angle and energy distributions of the atoms were calculated using the simulation model (see Section 2.1). At least 320000 atoms were used to simulate the deposition process based on the model described in Section 2.2. The atomic deposition rates were same with that in the experiment, and the environment temperature was 300 K. The substrate was assumed to be smooth, and the inclination angles investigated were the same as those used in the experiments (0, 20, 40, 50, 60, and 70°).

Optics EXPRESS

3. Experimental setup

An FJL600 DC magnetron sputtering system was used in this study. The vacuum system of this machine uses turbo molecular pumps, and the working gas is Ar gas. The environment temperature was kept at 300 K, the background pressure at $1.2e^{-3}$ Pa, and the working pressure at $6e^{-2}$ Pa. The substrates used were made of super-polished Si and had dimensions of 15 mm × 15 mm. The purities of the target Mo and Si are 99.95% and 99.999% respectively, and the targets are both produced by Umicore. The period of the deposited Mo/Si multilayer coatings was 40.5, meaning that the first and last layers were both of Si. Seven different inclination angles were evaluated, and the investigated range included both high and low angles as well as those that lay in between (0, 20, 30, 40, 50, 60, and 70°). The deposition rates at different substrate inclination angles are shown in Table 1. The Mo/Si multilayer coatings were deposited under the above-described process conditions. The surface roughness, structures, periodic thicknesses, and reflectivity of the coatings were evaluated using AFM, TEM, X-ray diffraction (XRD) machine, and ultraviolet spectrometer spectrometry, respectively.

Table 1. Experimental deposition rates at different substrate inclination angles.

Deposition atom	Deposition rates nm/s						
	0°	20°	30°	40°	50°	60°	70°
Mo	0.141	0.133	0.121	0.1053	0.0878	0.0695	0.0475
Si	0.146	0.135	0.125	0.108	0.0905	0.0719	0.0492

4. Results and discussions

4.1. Surface roughness measurements

AFM was used to measure the surface contours of the deposited Mo/Si multilayer coatings. A region with dimensions of 2 μm × 2 μm was analyzed for each sample (Fig. 6), and the roughness (RMS) of this region was calculated (Fig. 7).

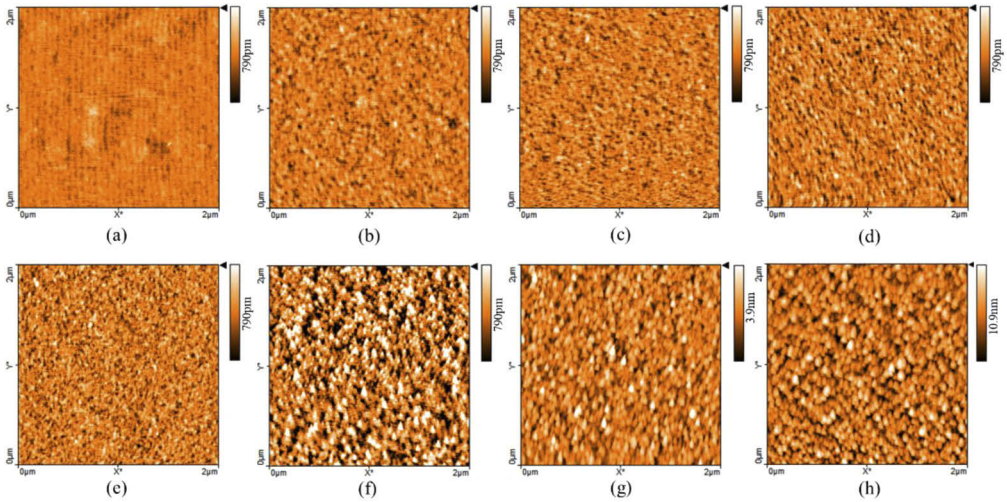

Fig. 6. Surface contour structures of experimental Mo/Si multilayer coatings deposited on substrates inclined at different angles: (a) uncoated substrate and substrates coated when inclined at angles of (b) 0, (c) 20, (d) 30, (e) 40, (f) 50, (g) 60, and (h) 70°.

Optics EXPRESS

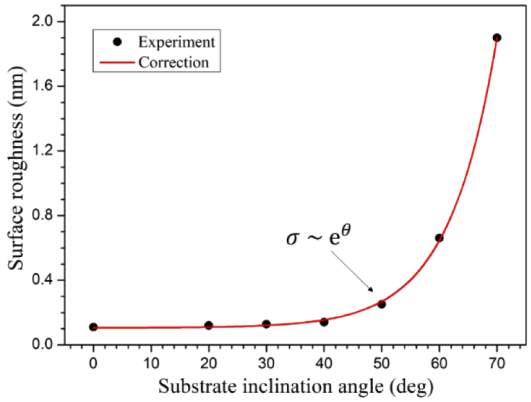

Fig. 7. Correlation between experimental surface roughness and inclination angle of substrate.

It can be observed that the surface roughness (RMS) of the uncoated super-polished substrate was quite small. However, granules formed on the substrate surface, and its roughness increased after the deposition of the coating. Nevertheless, the changes in the surface contours were small, and the surface roughness increased only slightly for inclination angles between 0° and 40°. On the other hand, the size of the surface granules as well as the surface roughness increased rapidly for inclination angles between 50° and 70°. Moreover, the experimentally determined surface roughness values were found to be exponentially correlated to the substrate inclination angle (see Fig. 7); in the figure, the black dots are the measured surface roughness, while the red curve is the fitted curve. The relationship can be expressed as follows:

$$\sigma = 4 \times 10^{-4} e^{\theta/8.33} + 0.105 \tag{1}$$

where σ is the surface roughness of the deposited coating and θ is the inclination angle of the substrate.

The surface roughness during the simulations were similar to those observed during the experiments (Fig. 8). In other words, in both cases, they exhibited an exponential relationship with the substrate inclination angle. The maximum deviation between the simulated and experimentally measured surface roughness was less than 20%, which means that the proposed simulation model is effective for calculating the surface roughness of Mo/Si multilayer coatings and study the changes in the surface roughness with the substrate inclination angle.

4.2. Power spectral density measurements

To accurately characterize the surface profile and provide a quantitative description of the spatial frequency distribution, it is necessary to introduce the evaluation method of PSD. The obtained surface contour information (shown in Fig. 6) can be converted to a spatial-frequency domain by Fourier transform. Because of the required infinite continuous range of Fourier transform, it cannot be used to calculate PSD directly. Therefore, the discretization method proposed by Stearns [37] was used for calculating the PSD.

$$PSD(v) = \frac{\Delta x}{M}\left|\sum_{m=0}^{M-1} z(m) w_{2k}(m) e^{-2\pi j(mvM)}\right|^2 \tag{2}$$

Here, Δx is the separation between the samples to ensure a correct dimension, M is the number of sampling points, $z(m)$ is a discrete form of the surface profile height function, v is the spatial frequency, and $w_{2k}(m)$ is the correction function.

Optics EXPRESS

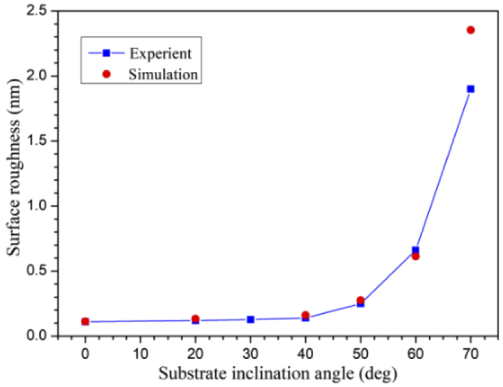

Fig. 8. Surface roughness (RMS) for substrate inclination angles of 0, 20, 40, 50, 60, and 70° as observed during simulations and experiments.

The PSD values for the different substrate inclination angles are shown in Fig. 9. It can be seen from the figure that both the high spatial frequency and the low spatial frequency surface roughness values of the various coatings were higher than those of the substrate. The low spatial frequency surface roughness remained almost unchanged, while the high spatial frequency surface roughness increased when the substrate inclination angle was increased from 0° to 20°. This meant that the size of the surface granules remained almost constant while their number density increased with the increase in the inclination angle. Further, both the low spatial frequency and the high spatial frequency surface roughness were similar at 20° and 40°. However, when the substrate inclination angle was increased from 40° to 50°, the high spatial frequency surface roughness remained almost unchanged but the low spatial frequency surface roughness increased sharply. This indicated that the size of the surface granules increased sharply with the increase in the inclination angle. Furthermore, the high spatial frequency and low spatial frequency surface roughness both increased significantly when the substrate inclination angle was increased from 50° to 70°. This was because, in this case, the deposited atoms were incident on the substrate surface at a very high angle. Hence, the energy transferred to the substrate was too low for kinetic energy assisted diffusion to occur [24,29–31]. Thus, island-like structures formed on the surface. Furthermore, owing to the large incident angle and the presence of these island-like structures, a blocking effect occurred, which led to the formation of even more island-like structures.

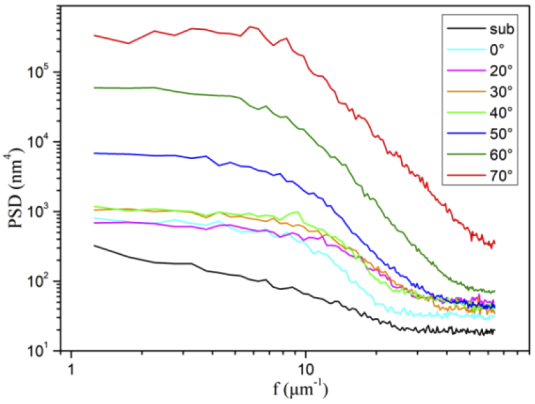

Fig. 9. PSD values of experimental Mo/Si multilayer coatings for different substrate inclination angles.

Optics EXPRESS

4.3. Periodic thickness measurements

Based on the results of the XRD measurement (Fig. 10), the periodic thicknesses of the multilayer coatings formed for substrate inclination angles of 0, 20, 40, and 50° were determined to be 7.0654, 6.9935, 6.8467, and 6.8054 nm, respectively. The fitted ratios (Mo fraction in the multilayer period) were all around 0.4. However, only a single diffraction peak was observed on the left side of the spectrum when the substrate inclination angle was 70° (see the red curve in Fig. 10). This indicated that the periodicity of this coating had been destroyed owing to the high substrate inclination angle.

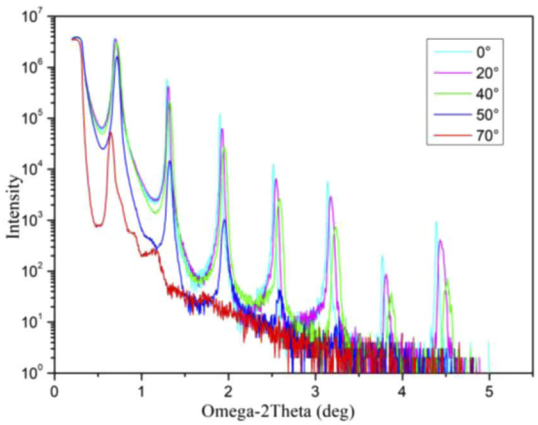

Fig. 10. XRD patterns of experimental Mo/Si multilayer coatings for different substrate inclination angles.

4.4. Analysis of coating structure

The structures of the Mo/Si multilayer coatings with period of 40.5 (the period is 20.5 in 70°) obtained from the simulations are shown in Fig. 11, where the red and blue layers represent the Mo and Si atoms, respectively.

TEM was performed to evaluate the structures of the Mo/Si multilayer coatings fabricated in experiments for substrate inclination angles of 0, 50, and 70° (Fig. 12). To allow for better visualization, magnified images of the Mo/Si multilayer coatings are shown in Fig. 13.

The following conclusions can be made based on the results shown in the figures:

(1) When the substrate inclination angle is 0, 20, 40, or 50°, a periodic Mo/Si multilayer coating is formed (Figs. 11–13). Further, the interface roughness between the Mo and Si layers increases with the increase in the substrate inclination angle. This is because the incident angle increases with the increase in the substrate inclination angle (from Figs. 2 and 3), and the block effect becomes more pronounced during deposition, resulting in an increase in the interface roughness. However, when the substrate inclination angle is 60 or 70°, the multilayer coating formed is not periodic. This is because the block effect is very strong and destroys the periodicity.

(2) Small imperfections are propagated throughout the individual interfaces (as descripted by the orange line in Fig. 14) when the substrate inclination angle is 40 or 50°. Macleod [38,39] stated that the multilayer growth angle, β, and incident angle, α, satisfy the expression $tan\beta = c\ \ tan\alpha$ ($c = 0.5$) when α is 40°, meaning that β is 23°. β was found to be approximately 20° when α was 40° during the simulations, in keeping with the results reported by Macleod. Furthermore, β was found to be approximately 40° when α was

Optics EXPRESS

50°; this was the case both during the simulations and the experiments. In the case too, the expression $tan\beta = c\ \ tan\alpha$ held true but with a higher c ($c = 0.7$), indicating that c increases with the incident angle.

4.5. Reflectivity measurements

The extreme ultraviolet spectrometry was used to measure the reflectivity of the Mo/Si multilayer coatings in the EUV band. For the substrate inclination angle of 0°, the peak reflectivity is 65.13%. The normalized peak reflectivity (relative to 0°) of the Mo/Si multilayer deposited for substrate inclination angles of 0, 20, 40, 50, and 60° are shown in Fig. 15. The peak reflectivity decreases only slightly when the substrate inclination angle is increased from 0° to 20° and then

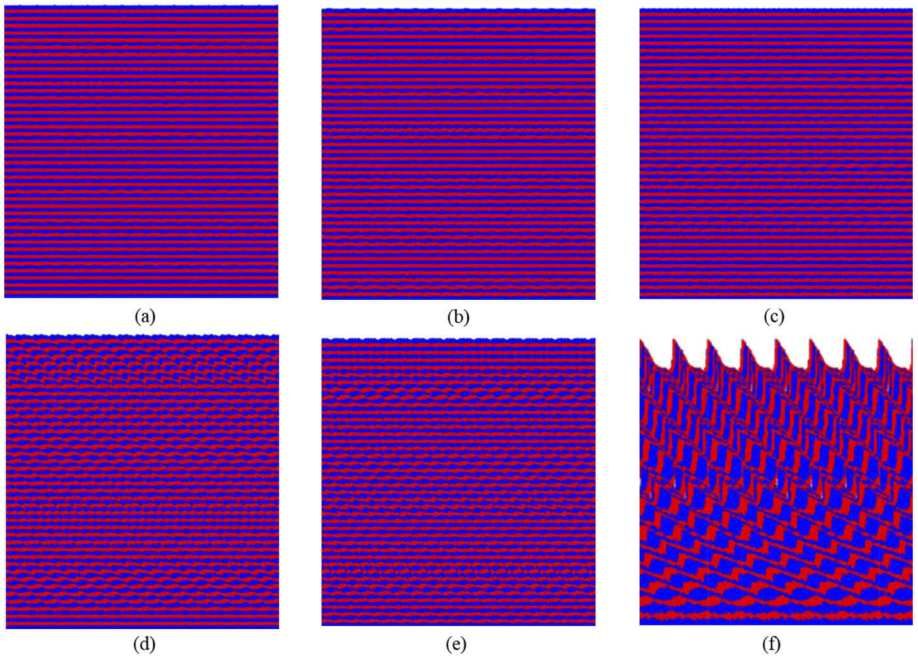

Fig. 11. Simulated structures of multilayer coatings with period of 40.5 at different substrate inclination angles as determined through simulations: (a) 0, (b) 20, (c) 40, (d) 50, (e) 60, and (f) 70° (the period is 20.5).

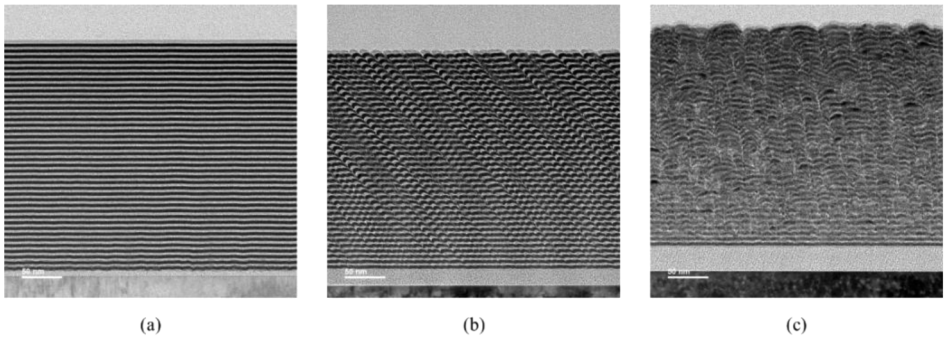

Fig. 12. Experimental TEM Images of Mo/Si multilayer coatings for substrate inclination angles of (a) 0°, (b) 50°, and (c) 70°.

Optics EXPRESS

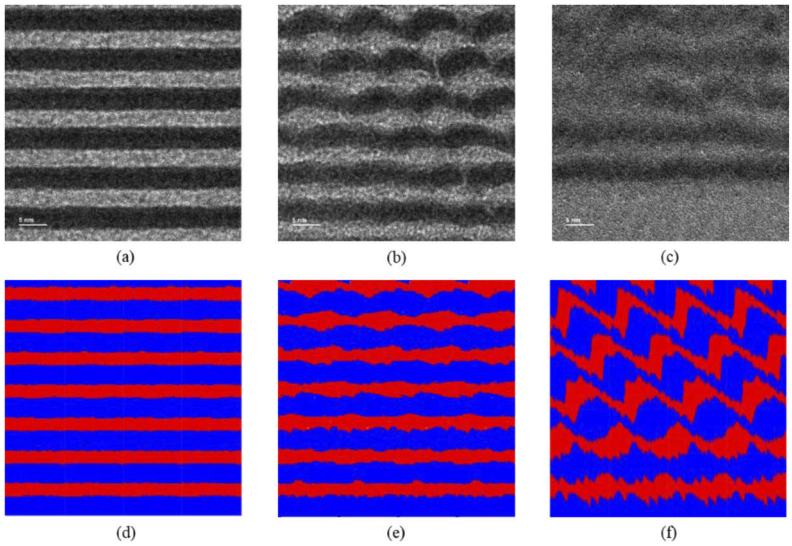

Fig. 13. Magnified images of structures of multilayer coatings at substrate inclination angles of (a) 0°, (b) 50° and (c) 70° as determined through experiments and (d) 0°, (e) 50° and (f) 70° in simulations

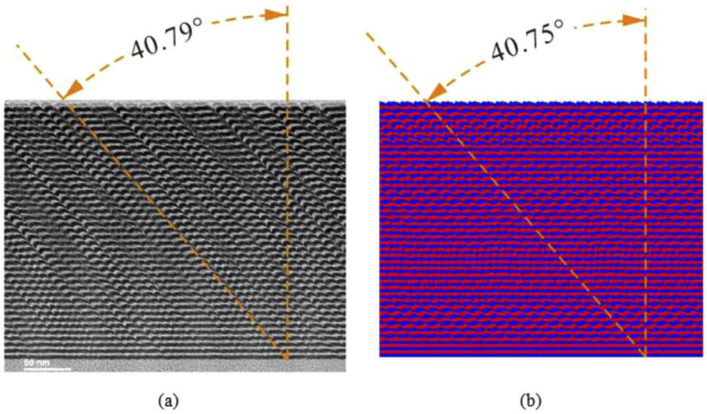

Fig. 14. Propagation of small imperfections throughout individual interfaces at substrate angle of 50° as observed during (a) experiments and (b) simulations.

to 40°. However, the peak reflectivity decreases sharply, falling to less than 0.54 at 50° and decreases further to 0.17 at 60°. This is in keeping with the results of the AFM and PSD analysis, which suggested that the size of the surface granules and hence the surface roughness increases with the inclination angle, as well as the TEM results, which showed that irregular interfaces are formed when the substrate inclination angle is greater than 40°. It can be further inferred that the reflectivity is nearly 0 at the substrate angle of 70° owning to the significant surface roughness and destruction of periodic structures.

4.6. Discussions

We have developed a model for explaining the increase of interfacial roughness of Mo/Si multilayers with the increase of substrate inclination angle. Our goal is not only to explain things

Optics EXPRESS

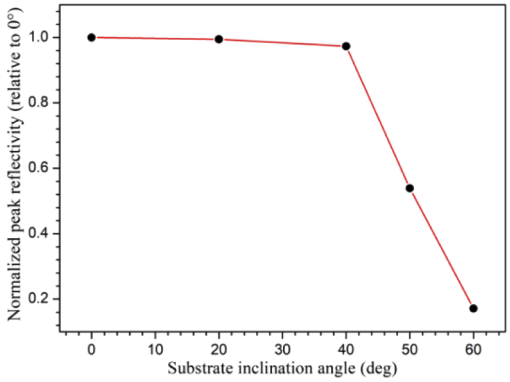

Fig. 15. Normalized peak reflectivity of Mo/Si multilayer coatings for substrate inclination angles of 0, 20, 40, 50, and 60°

but also to improve things. It is well known that the interfacial roughness of Mo/Si multilayers can be reduced by polishing the surface of Si layer [13,14]. The established model can simulate this kinetic energy assisted diffusion processes and tune the flux, incident angle and energy of Ar^+ to decrease the interface roughness.

Using the proposed model, we simulate the Mo/Si multilayers with 10 bi-layers at substrate inclination angles of 20, 40, and 50° under two conditions: 1) unpolished; 2) Si layers polished by Ar^+. Figure 16 shows that the interface is smoothed apparently after Si layers are polished by Ar^+. Figure 17(a) implies that the surface roughness (RMS) all decrease at different inclination angles when Si layers are polished by Ar^+. Figure 17(b) shows that the etched thicknesses of Si layer polished by Ar^+ are different at different inclination angles. The simulation results indicate that the deterioration of interfacial roughness with larger inclination angles can be compensated by the polish of Si layer with different etched thicknesses. As to the experimental implement, the etched thickness distribution of Si layer for different part of collector can be controlled by modulating the velocity of substrate sweeping across the ion source.

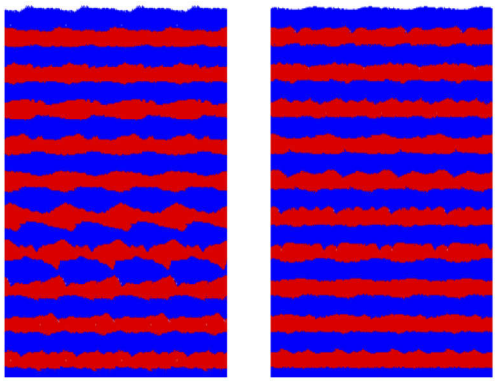

Fig. 16. Simulated structures of the Mo/Si multilayers with 10 bi-layers at substrate inclination angle of 50°, (a) unpolished, (b) Si layers polished by Ar^+, the etched thickness of Si layer is 0.91nm, incident angle and energy of Ar^+ are 50° and 50eV.

Optics EXPRESS

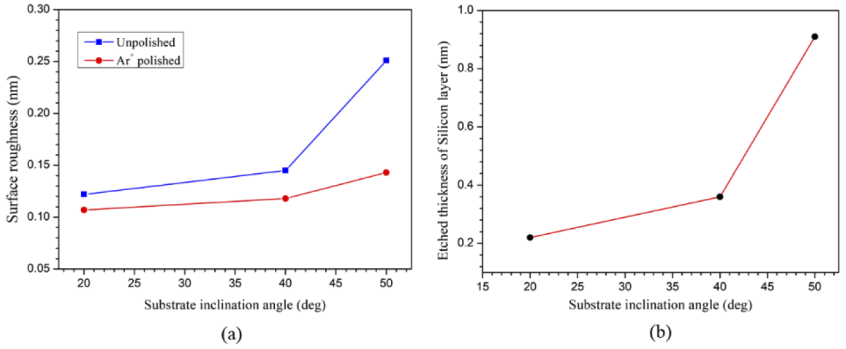

Fig. 17. (a) Simulated surface roughness (RMS) of Mo/Si multilayers at different inclination angles (unpolished and Ar^+ polished), (b) etched thickness of Si layer at different inclination angles.

5. Conclusions

In this work, Mo/Si multilayer coatings with a period of 40.5 were fabricated, and a model was developed to simulate the deposition process of the coatings based on the high-energy and thermal diffusion physical processes. The primary focus was the changes in the surface and interface roughness, layer structure, and coating reflectivity of the multilayer coatings with changes in the substrate inclination angle, and a total of seven different angles (0, 20, 30, 40, 50, 60, and 70°) were studied. The main findings of the study can be summarized as follows:

(1) For substrate inclination angles smaller than 40°, the surface and interface roughness of the multilayer coatings increases slightly with an increase in the inclination angle, and the layers are kept periodic. However, for substrate inclination angles greater than 40°, the surface and interface roughness increase sharply with increases in the inclination angle, further, the layers become irregular and the periodicity is destroyed at very large inclination angles (60 and 70°). Further, the relationship between the surface roughness and substrate inclination angle is an exponential one.

(2) For substrate inclination angles lower than 40°, the reflectance of the multilayer coatings with respect to EUV decreases slightly with an increase in the inclination angle. However, for substrate inclination angles greater than 40°, the reflectance with respect to EUV decreases sharply with the increase in the inclination angle. In addition, it was also found that the high roughness of the coating surface and interfaces are responsible for the significant decrease in the reflectance at large inclination angles. Thus, it is essential to improve the coating process in order to increase the reflectance at large inclination angles.

(3) On comparing the surface roughness results of the experiments and simulations, it was found that the deviation in the roughness was less than 20%. This confirmed the effectiveness of proposed model. Furthermore, the proposed deposition model could serve as a theoretical basis for the advanced coating process development.

Funding

National Natural Science Foundation of China (61605201, 21603211).

Acknowledgments

The authors acknowledge the TEM facilities, the scientific, and technical assistance, of Materials Analysis Technology (Shanghai) Ltd.

Optics EXPRESS

Disclosures

The authors declare no conflicts of interest.

References

1. D. Attwood and S. Anne, *Soft x-rays and extreme ultraviolet radiation: Principles and applications* (Cambridge University, 2000).
2. E. Louis, A. E. Yakshin, T. Tsarfati, and F. Bijkerk, "Nanometer interface and materials control for multilayer EUV-optical applications," Prog. Surf. Sci. **86**(11-12), 255–294 (2011).
3. C. Wagner and N. Harned, "Lithography gets extreme," Nat. Photonics **4**(1), 24–26 (2010).
4. D. C. Brandt, I. V. Fomenkov, A. I. Ershov, W. N. Partlo, D. W. Myers, N. R. Böwering, A. N. Bykanov, G. O. Vaschenko, O. V. Khodykin, and J. R. Hoffman, "LPP EUV source development for HVM," Proc. SPIE 6517, 65170Q (2007).
5. B. Yu, C. Jin, S. Yao, C. Li, H. Wang, F. Zhou, B. Guo, Y. Xie, Y. Liu, and L. Wang, "Control of lateral thickness gradients of Mo–Si multilayer on curved substrates using genetic algorithm," Opt. Lett. **40**(17), 3958–3961 (2015).
6. B. Yu, L. Wang, H. Li, Y. Xie, H. Wang, H. Zhang, S. Yao, Y. Liu, J. Yu, C. Li, C. Xie, and C. Jin, "Low-stress and high-reflectance Mo/Si multilayers for EUVL by magnetron sputtering deposition with bias assistance," Proc. SPIE 10583, 105831T (2018).
7. H. Mizoguchi, H. Nakarai, T. Abe, K. M. Nowak, Y. Kawasuji, H. Tanaka, and T. Yanagida, "High power LPP-EUV source with long collector mirror lifetime for high volume semiconductor manufacturing," in *Proceedings of IEEE Conference on China Semiconductor Technology International Conference* (IEEE, 2018), pp. 1–7.
8. M. Kriese, Y. Platonov, B. Ehlers, L. Jiang, and T. Lucatorto, "Development of an EUVL collector with infrared radiation suppression," Proc. SPIE **9048**, 90483C (2014).
9. T. Feigl, M. Perske, H. Pauer, T. Fiedler, S. Yulin, N. Kaiser, A. Tünnermann, N. R. Böwering, A. I. Ershov, S. d. Dea, K. Hoffmann, B. L. Fontaine, I. V. Fomenkov, and D. C. Brandt, "Lifetime and refurbishment of multilayer LPP collector mirrors," Proc. SPIE 8679, 86790C (2013, April).
10. D. M. Broadway, Y. Y. Platonov, and L. A. Gomez, "Achieving desired thickness gradients on flat and curved substrates," Proc. SPIE 3766, 262–274 (1999).
11. J. D. Torre, G. H. Gilmer, D. L. Windt, R. Kalyanaraman, F. H. Baumann, P. L. O'Sullivan, J. Sapjeta, T. D. de la Rubia, and M. Djafari Rouhanil, "Microstructure of thin tantalum films sputtered onto inclined substrates: Experiments and atomistic simulations," J. Appl. Phys. **94**(1), 263–271 (2003).
12. D. L. Voronov, P. Gawlitza, S. Braun, and H. A. Padmore, "Spontaneous formation of highly periodic nano-ripples in inclined deposition of Mo/Si multilayers," J. Appl. Phys. **122**(11), 115303 (2017).
13. R. V. Medvedev, K. V. Nikolaev, A. A. Zameshin, D. IJpes, I. A. Makhotkin, S. N. Yakunin, A. E. Yakshin, and F. Bijkerk, "Low-energy ion polishing of Si in W/Si soft X-ray multilayer structures," J. Appl. Phys. **126**(4), 045302 (2019).
14. S. Braun, P. Gawlitza, M. Menzel, W. Friedrich, J. Schmidt, and A. Leson, "Specific aspects of roughness and interface diffusion in non-periodic Mo/Si multilayers," Proc. SPIE 9207, 920707 (2014, September).
15. N. Metropolis, A. W. Rosenbluth, M. N. Rosenbluth, and A. H. Teller, "Equation of state calculations by fast computing machines," J. Chem. Phys. **21**(6), 1087–1092 (1953).
16. Y. G. Yang, R. A. Johnson, and H. N. G. Wadley, "A Monte Carlo simulation of the physical vapor deposition of nickel," Acta Mater. **45**(4), 1455–1468 (1997).
17. M. Schneider, A. Rahman, and I. K. Schuller, "Role of relaxation in epitaxial growth: A molecular-dynamics study," Phys. Rev. Lett. **55**(6), 604–606 (1985).
18. J. Roth, B. Josef, and W. Ottenberger, "Data on low energy light ion sputtering," *Max-Planck-Institut für Plasmaphysik. Report IPP* 9(26), (1979).
19. Y. Yamamura and K. Muraoka, "Over-cosine angular distributions of sputtered atoms at normal incidence," Nucl. Instrum. Methods Phys. Res., Sect. B **42**(2), 175–181 (1989).
20. J.F. Ziegler, "The Transport of Ions in Matter," Nucl. Instr. Methods Phys. Res. Sect. B **1027**, 219–220 (1991).
21. J. P. Biersack and L. G. Haggmark, "A Monte Carlo computer program for the transport of energetic ions in amorphous targets," Nucl. Instrum. Methods **174**(1-2), 257–269 (1980).
22. W. Eckstein, *Computer Simulation of Ion-Solid Interactions* (Springer, Berlin Heidelberg, 2013)
23. K. Van Aeken, S. Mahieu, and D. Depla, "The metal flux from a rotating cylindrical magnetron: a Monte Carlo simulation," J. Phys. D: Appl. Phys. **41**(20), 205307 (2008).
24. Y. G. Yang, X. W. Zhou, R. A. Johnson, and H. N. G. Wadley, "Monte carlo simulation of hyperthermal physical vapor deposition," Acta Mater. **49**(16), 3321–3332 (2001).
25. Y. Luo, M. Lin, N. Zhou, H. Huang, C. T. Tsai, and L. Zhou, "Molecular dynamics simulation study of the microstructure of a-Si: H thin film grown by oblique-angle deposition," Phys. B **545**, 80–85 (2018).
26. H. Huang, G. H. Gilmer, and T. D. de la Rubia, "An atomistic simulator for thin film deposition in three dimensions," J. Appl. Phys. **84**(7), 3636–3649 (1998).
27. X. W. Zhou and H. N. G. Wadley, "Hyperthermal vapor deposition of copper: reflection and resputtering effects," Surf. Sci. **431**(1-3), 58–73 (1999).

Optics EXPRESS

28. X. W. Zhou and H. N. G. Wadley, "Hyperthermal vapor deposition of copper: athermal and biased diffusion effects," Surf. Sci. **431**(1-3), 42–57 (1999).
29. W. Eckstein, Computer simulation of ion-solid interactions, (Springer Science & Business Media 1991), Vol. 10.
30. J. D. Kress, D. E. Hanson, A. F. Voter, C. L. Liu, X. Y. Liu, and D. G. Coronell, "Molecular dynamics simulation of Cu and Ar ion sputtering of Cu (111) surfaces," J. Vac. Sci. Technol., A **17**(5), 2819–2825 (1999).
31. D. E. Hanson, J. D. Kress, A. F. Voter, and X. Y. Liu, "Trapping and desorption of energetic Cu atoms on Cu (111) and (001) surfaces at grazing incidence," Phys. Rev. B **60**(16), 11723–11729 (1999).
32. M. S. Daw and M. I. Baskes, "Semiempirical, quantum mechanical calculation of hydrogen embrittlement in metals," Phys. Rev. Lett. **50**(17), 1285–1288 (1983).
33. M. S. Daw and M. I. Baskes, "Embedded-atom method: Derivation and application to impurities, surfaces, and other defects in metals," Phys. Rev. B **29**(12), 6443–6453 (1984).
34. M. I. Baskes, "Modified embedded-atom potentials for cubic materials and impurities," Phys. Rev. B **46**(5), 2727–2742 (1992).
35. G. Henkelman, B. P. Uberuaga, and H. Jónsson, "A climbing image nudged elastic band method for finding saddle points and minimum energy paths," J. Chem. Phys. **113**(22), 9901–9904 (2000).
36. M. Villarba and H. Jónsson, "Low-temperature homoepitaxial growth of Pt (111) in simulated vapor deposition," Phys. Rev. B **49**(3), 2208–2211 (1994).
37. D. G. Stearns, D. P. Gaines, D. W. Sweeney, and E. M. Gullikson, "Nonspecular x-ray scattering in a multilayer-coated imaging system," J. Appl. Phys. **84**(2), 1003–1028 (1998).
38. J. M. Nieuwenhuizen and H. B. Haanstra, "Microfractography of thin films," Philips Tech. Rev. **27**(3), 87–91 (1966).
39. H. A. Macleod, "Structure-related optical properties of thin films," J. Vac. Sci. Technol., A **4**(3), 418–422 (1986).